

Can we observe the many-body localization?

Piotr Sierant^{1,2} and Jakub Zakrzewski^{2,3,*}

¹The Abdus Salam International Center for Theoretical Physics, Strada Costiera 11, 34151, Trieste, Italy

²Institute of Theoretical Physics, Jagiellonian University in Kraków, Lojasiewicza 11, 30-348 Kraków, Poland

³Mark Kac Complex Systems Research Center, Jagiellonian University in Krakow, Kraków, Poland.

(Dated: September 29, 2021)

We study time dynamics of 1D disordered Heisenberg spin-1/2 chain focusing on a regime of large system sizes and a long time evolution. This regime is relevant for observation of many-body localization (MBL), a phenomenon that is expected to freeze the dynamics of the system and prevent it from reaching thermal equilibrium. Performing extensive numerical simulations of the imbalance, a quantity often employed in the experimental studies of MBL, we show that the regime of a slow power-law decay of imbalance persists to disorder strengths exceeding by at least a factor of 2 the current estimates of the critical disorder strength for MBL. Even though we investigate time evolution up to few thousands tunneling times, we observe no signs of the saturation of imbalance that would suggest freezing of system dynamics and provide a smoking gun evidence of MBL. We demonstrate that the situation is qualitatively different when the disorder is replaced by a quasiperiodic potential. In this case, we observe an emergence of a pattern of oscillations of the imbalance that is stable with respect to changes in the system size. This suggests that the dynamics of quasiperiodic systems remain fully local at the longest time scales we reach provided that the quasiperiodic potential is sufficiently strong. Our study identifies challenges in an unequivocal experimental observation of the phenomenon of MBL.

I. INTRODUCTION

Generic isolated quantum many-body systems initialized in an out-of-equilibrium state are expected to approach featureless thermal states described by the eigenstate thermalization hypothesis [1–3]. Many-body localization (MBL) [4, 5] has been put forward as a mechanism that prevents the approach to equilibrium due to an interplay of interactions and strong disorder.

The phenomenon of MBL has received a lot of attention over the last decade [6–8]. The MBL phase is characterized by presence of local integrals of motion [9–15] that inhibit the transport [6, 16], and slow down the spreading of the quantum entanglement [17, 18]. MBL has been investigated numerically in disordered spin chains [19–22] that map onto spinless fermionic chains, in systems of spinful fermions [23–26] or bosons [27–29] and found in systems with random interactions [30–32] or in various types of quasiperiodic systems [33–35]. All those investigations were confirming the belief that MBL is a robust mechanism of ergodicity breaking, that can be expected to occur in a wide class of local, one-dimensional quantum many-body systems provided that a sufficiently strong quenched disorder is present.

This belief was challenged in [36] where it was argued that MBL might not be stable in the asymptotic sense, i.e. in the limit of an infinite time and system size, and the observations of earlier works indicate only a presence of an MBL regime found at a finite system size and finite times. This led to an intense debate about the stability of MBL [37–39] and its dynamical properties [40–43]. Despite these works, it is presently unclear whether a stable

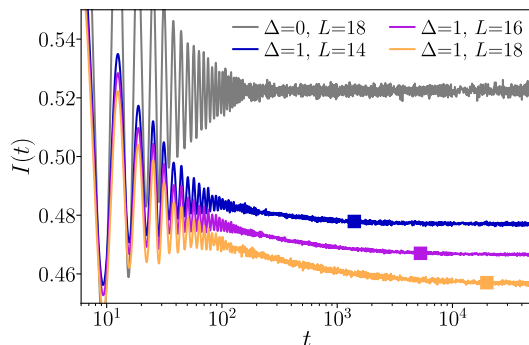


FIG. 1. Interactions induce a slow but persistent to long times decay of the imbalance $I(t)$ as visible from the comparison of results for non-interacting ($\Delta = 0$) and interacting ($\Delta = 1$) system. Data for disordered XXZ model (1) at disorder strength $W = 4$. The squares denote the Heisenberg time t_H that scales exponentially with system size L .

MBL phase exists much deeper in the MBL regime than it was previously estimated [44] or whether there is no stable MBL phase at all. An example of the latter scenario is provided by disordered constrained spin chains which, despite hosting a wide non-ergodic regime at finite system sizes [45] become ergodic in the thermodynamic limit [46].

The double limit of infinite time and system size lies at the source of difficulties in establishing the status of MBL. On one hand, one may investigate properties of eigenstates of many-body systems, that encode the properties of the system at infinite time. However, the eigenstates can be found in an unbiased fashion only for relatively small system sizes L (for instance, for the usually studied spin-1/2 chains, $L \leq 24$ [47, 48]), which does not allow for a fully controlled extrapolation of the results to

* jakub.zakrzewski@uj.edu.pl

the thermodynamic limit $L \rightarrow \infty$. On the other hand, tensor network algorithms [49, 50] such as TEBD [51, 52] or TDVP [53–55] allow one to study time evolution of systems comprised of hundreds or even thousands of sites. Unfortunately, the time evolution of many-body systems can be traced faithfully with such algorithms only up to times restricted by the growth of the entanglement in the system. Since, in strongly disordered systems, the entanglement entropy grows only logarithmically in time, maximal times of several hundred tunneling times were achieved in [25, 56–58]. Nevertheless, there is no straightforward way of extrapolating these results to the infinite time limit.

Fig. 1 illustrates the difficulties in assessing whether the system is ergodic or MBL in a quench experiment. It shows the time evolution of the so-called imbalance $I(t)$ for a disordered XXZ spin-1/2 chain (precise definitions are given in the following section). An ergodic system has no memory of its initial state and the imbalance vanishes in the long-time limit: $I(t) \xrightarrow{t \rightarrow \infty} 0$. In contrast, the information about the initial density profile persists indefinitely in the MBL phase in which $I(t) \xrightarrow{t \rightarrow \infty} I_0 > 0$. For the non-interacting system ($\Delta = 0$) one clearly sees that after initial oscillations, the imbalance saturates to a constant value. Such a behavior allows for a straightforward experimental observation of Anderson localization in the absence of interactions [59, 60]. The main effect of interactions is that the imbalance decays to much longer times, as exhibited by data for $\Delta = 1$. The time scale at which $I(t)$ ceases to decay is of the order of Heisenberg time t_H that is proportional to an inverse of the mean level spacing of the system and hence it is exponentially large in the system size L . In a consequence, the data presented in Fig. 1 allow us only to conclude that at the considered disorder strength $W = 4$, the system is in a MBL regime. The value of the imbalance in the $t \rightarrow \infty$ limit is clearly decreasing with system size L and it is impossible to determine from data in Fig. 1 whether in the $L \rightarrow \infty$ the system remains MBL at $W = 4$ or whether the ergodicity is restored.

This explains the title of our work: Can we observe the many-body localization? The presence of MBL regime has been demonstrated in a number of numerical works as well as in experiments with cold atoms and ions [61–67]. The aim of this work is to determine whether we can observe unambiguous signatures of the MBL phase in the time evolution of disordered many-body systems. To that end we perform extensive numerical simulations of disordered XXZ spin-1/2 chain and concentrate on the time evolution of density correlation functions.

Let us note that we on purpose limit our discussion to short-ranged interactions although MBL has been addressed also for long-range (e.g. dipolar [68–72], Ising-type [73–75] or cavity-mediated [76, 77]) interactions. Similarly we do not address the existence and properties of localization in disorder-free potentials (such as e.g. tilted lattices) - the subject of intensive recent studies [78–91]. We want to concentrate on the “pure”, tradi-

tional MBL case.

The paper is structured as follows. In Sec. II we introduce the XXZ spin chain. We provide results for small system sizes and formulate tentative criteria for observation of MBL phase in Sec. III. Then, we verify whether those criteria are fulfilled by dynamics of the XXZ spin chain in the regime of large disorder strengths and system sizes in Sec. IV. Subsequently, we investigate time evolution of entanglement entropy in that regime in Sec. V. Finally, instead of random disorder we consider time dynamics of the system with a quasiperiodic potential in Sec. VI. We draw our conclusions in Sec. VII.

II. MODEL AND OBSERVABLES

In this work we concentrate on 1D XXZ spin chain with Hamiltonian given by

$$H = J \sum_{i=1}^L (S_i^x S_{i+1}^x + S_i^y S_{i+1}^y + \Delta S_i^z S_{i+1}^z) + \sum_{i=1}^L h_i S_i^z \quad (1)$$

where \vec{S}_i are spin-1/2 matrices, $J = 1$ is fixed as the energy unit, open boundary conditions are assumed and $h_i \in [-W, W]$ are independent, uniformly distributed random variables. The Jordan-Wigner transformation allows to map XXZ spin chain (1), to a system of interacting spinless fermions, with the tunneling matrix element equal to J and nearest-neighbor interaction strength Δ . This allows to make connection between disordered XXZ model and optical lattice experiments (as e.g. in [61]). The random-field XXZ spin chain has been widely studied in the MBL context, see e.g. [22, 92–100]. Various estimates of the critical disorder strength W_C for the transition to MBL phase include: $W_C \approx 3.7$ [22], $W_C \approx 3.8$ [101], $W_C \approx 4.2$ [57, 102], $W_C \gtrsim 5$ [56, 103], $W_C \approx 5.4$ [48].

Besides the random disorder $h_i \in [-W, W]$, we also consider the case of quasiperiodic (QP) potential, for which $h_j = W^{\text{QP}} \cos(2\pi kl + \phi)$, where $k = (\sqrt{5}-1)/2$ and ϕ is a random phase taken from the uniform distribution between $[0, 2\pi]$. The QP potential breaks the translation invariance of the system playing a role similar to disorder and leading to MBL at a critical strong amplitude of the QP potential W_C^{QP} , with various estimates ranging from $W_C^{\text{QP}} \approx 1.5$ [33, 104–108] through $W_C^{\text{QP}} \approx 2.4$ [109, 110], up to $W_C^{\text{QP}} \approx 4$ [111]. Its important to note that the properties of the transition to MBL phase in QP systems are distinct from the transition in system with random disorder [34, 112–114].

We analyze dynamics of imbalance

$$I(t) = D \sum_{i=1+l_0}^{L-l_0} \langle \psi(t) | S_i^z | \psi(t) \rangle \langle \psi | S_i^z | \psi \rangle, \quad (2)$$

where $|\psi(t)\rangle = e^{-iHt}|\psi\rangle$, $|\psi\rangle$ is the initial state, the constant D assures that $I(0) = 1$, $l_0 > 0$ diminishes

the influence of boundaries (in our calculations we take $l_0 = 2$). The results are averaged over n_{real} disorder realizations. As the initial state we take the Néel state with every second spin pointing up and every second spin down $|\psi\rangle = |\uparrow\downarrow\dots\uparrow\downarrow\rangle$. In the following Section we also take $|\psi\rangle$ as a product state of eigenstates of S_i^z operators with average energy $\langle\psi|H|\psi\rangle$ being in the middle 10% of the spectrum of H – we refer to such a choice as to a density correlation function $C(t)$.

We note that other observables, see e.g. [96, 115], suffer from finite size and finite time limitations similar as (2). Hence, it seems that their behavior is always governed by the broad distributions of relaxation time scales [116], and that is why we concentrate on the very simple observable given by (2), which has another advantage of being directly accessible in experiments with cold atoms [61].

To find the time evolved state $|\psi(t)\rangle$ we employ Chebyshev expansion of the evolution operator e^{-iHt} [117], which allows us to investigate time evolution of systems of $L \leq 20$ sites up to the Heisenberg time $t_H = 2\pi/\bar{s} \sim e^{cL}$ (where \bar{s} is the average level spacing in the middle of the spectrum). For larger system sizes $L = 50, 100, 200$ we use a TDVP algorithm [53–55], with bond dimension χ , specified later in the text for each W and L considered. In the latter case we focus on relatively large disorder strengths $W \geq 8$ which allows us to investigate time evolution up to a few thousand tunneling times J^{-1} .

III. HOW TO OBSERVE AN MBL PHASE?

Numerical [118] as well as experimental [63] investigations of the imbalance $I(t)$ indicate a presence of a wide regime of disorder strength W in which the imbalance decays according to a power-law $I(t) \sim t^{\bar{\beta}}$. As a criterion for a transition to MBL, the work [56] introduced the condition that $\bar{\beta}$ vanishing within error bars implies the onset of MBL. The problem with such a criterion is that the error bars on $\bar{\beta}$ can be significantly reduced with increasing time of evolution and number of disorder samples, pushing the tentative boundary of MBL to larger and larger disorder strengths. An alternative was put forward in [58], which used a cut-off $\bar{\beta}_{\text{cut}}$ such that $\bar{\beta} < \bar{\beta}_{\text{cut}}$ implies MBL behavior. The cut-off value of $\bar{\beta}_{\text{cut}}$ was taken from a comparison of critical disorder strength estimated from gap ratio statistics as $W_C \approx 4$ for system size $L \approx 20$ and the decay rate of imbalance at that system size.

The latter criterion also runs into problems. If we assume a simplified model of the decay of the imbalance, in which $I(t) \sim t^{\bar{\beta}}$ for $t < t_H$, and then $I(t) = \text{const}$ for $t > t_H$ (which is mildly consistent with data shown in Fig. 1), then the value of the imbalance at infinite time is: $I(\infty) = I(t_H) = e^{-cL\bar{\beta}}$. Hence, in order to have a finite value of imbalance in the $t \rightarrow \infty$ the exponent governing decay of imbalance should vanish at least as $\bar{\beta} \sim L^{-1}$. Keeping this in mind we now examine the dynamics of

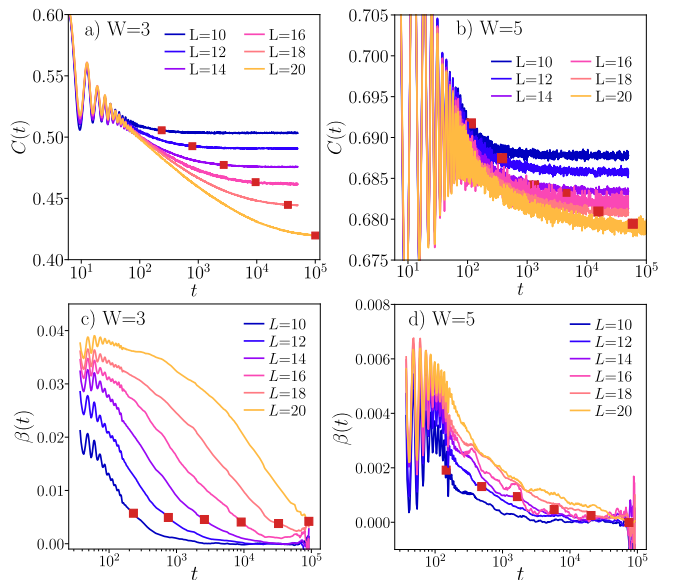


FIG. 2. Time evolution of density correlation function $C(t)$ in disordered XXZ model. Panels a) and b) – $C(t)$ for various system sizes $L = 10, \dots, L = 20$ at disorder strengths $W = 3, 5$, data averaged over $n_{\text{real}} > 10^4$ disorder realizations. Panels c) and d) – time evolution of the flowing beta function $\beta(t)$ that locally describes the exponent of decay of $C(t)$. The red squares denote the Heisenberg time $t_H \sim e^{cL}$.

the density correlation function $C(t)$ in a system of moderate size $L \leq 20$.

Fig. 2a) shows $C(t)$ for disorder $W = 3$ for which the XXZ spin chain is in the ergodic phase. With an increasing system size, the power-law decay of $C(t)$ persists to longer and longer times, not changing much beyond the Heisenberg time t_H . The interaction induced decay of $C(t)$ is evidently getting more abrupt with increasing L . The situation is, in fact quite similar for $W = 5$ (see Fig. 2b), which, according to the majority of estimates (e.g. [22, 35, 102]) is already in the MBL phase. While the decay of $C(t)$ is much slower than for $W = 3$, it persists to long-times and the saturation value of $C(t)$ is decreasing with L .

To investigate the slow decay of $C(t)$ in more quantitative fashion, we consider a time-dependent $\beta(t)$ function [109], that is obtained from the fit $C(t_1) = at_1^{-\beta(t)}$ in the interval $t \in [t_1, 1.5t_1]$. The resulting $\beta(t)$ functions are shown in Fig. 2 c),d). For $W = 3$ we observe that at first, the decay of $C(t)$ is well described by a power-law ($\beta(t)$ is constant) and then the decay gradually slows down, stopping at the time scale approximately order of magnitude larger than t_H . For $W = 5$, the slow down of the decay of $C(t)$ occurs at smaller times, however, a non-vanishing $\beta(t)$ up to Heisenberg time signals further, non-negligible decay of the density correlation function.

Results presented in this section show that the correlation functions decay up to Heisenberg time or even longer. Moreover, comparison of results for $W = 3$ and $W = 5$ indicates that it is hard to propose an accurate

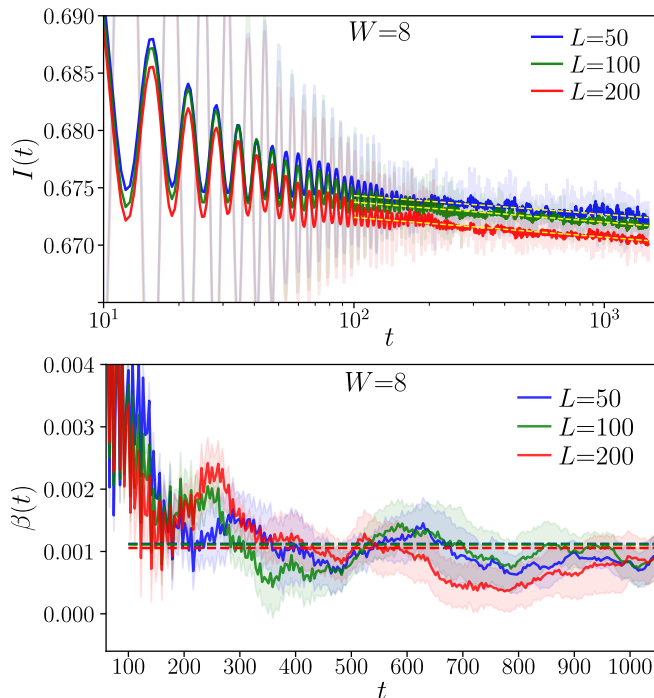


FIG. 3. Time evolution of imbalance $I(t)$ for systems of size $L = 50, 100, 200$ at disorder strength $W = 8$, details of the simulations and fits are given in Tab. I. Top: the shaded lines denote $I(t)$ whereas the solid lines denote a running average of $I(t)$ over window $(t-25, t+25)$, dashed lines denote power-law fits $I(t) \sim t^{-\bar{\beta}}$ in time interval $t \in [100, 1500]$. Bottom: the running beta function $\beta(t)$, dashed lines show the value of $\bar{\beta}$.

phenomenological model for the decay of $C(t)$. Nevertheless, building on intuitions obtained in this section, we conclude that an unambiguous observation of MBL phase should include at least one of the two conditions:

- (A) the value of the exponent $\bar{\beta}$ that is decreasing with system size as L^{-1} - in such a case even if the power-law decay persists up to the Heisenberg time, the imbalance is non-vanishing in the limit $t \rightarrow \infty$
- (B) a decrease of value of $\beta(t)$ that occurs in a system size independent fashion indicating the saturation of the imbalance beyond a certain time scale.

With those conditions in mind, we now turn to an analysis of time dynamics of large systems in the strong-disorder, long-time regime, which seems to be the most suitable one to find signatures of the *MBL phase*.

TABLE I. Details of numerical simulations for $W = 8$: system size L , maximal time reached in time evolution t_{\max} , the bond dimension χ , number of disorder realizations n_{real} , and the exponent $\bar{\beta}$ obtained from the fit $I(t) \sim t^{-\bar{\beta}}$ in interval $t \in [100, 1500]$.

	t_{\max}	χ	n_{real}	$\bar{\beta}$
$L=50$	1500	128	2000	$(10.5 \pm 0.5) \cdot 10^{-4}$
$L=100$	1500	128	2000	$(11.2 \pm 0.4) \cdot 10^{-4}$
$L=200$	1500	128	1000	$(11.1 \pm 0.4) \cdot 10^{-4}$

IV. TIME EVOLUTION OF IMBALANCE AT STRONG DISORDER IN LARGE SYSTEMS

Taking into account the various estimates of the critical disorder strength W_C for transition to MBL phase, discussed in Sec. II, we fix the disorder amplitude at $W = 8$ and $W = 10$. Such disorder strengths, according to the aforementioned estimates of W_C , are expected to lay significantly above the transition to the MBL phase.

The evolution of imbalance $I(t)$ for $W = 8$ is shown in Fig. 3 whereas the details of numerical simulations are shown in Tab. I. After an initial transient decay and oscillations that last up to $t \approx 100$, we observe a slow but steady monotonic decrease of $I(t)$ that persists up to the largest time $t_{\max} = 1500$ reached in the simulation. The value of t_{\max} is not sufficiently large to unambiguously pin-point the functional form of the decay of $I(t)$. Nevertheless, we observe that the imbalance is well fitted by a power-law decay $I(t) \sim t^{-\bar{\beta}}$ in the interval $t \in [100, 1500]$. The values of the exponent $\bar{\beta}$, shown in Tab. I, are positive confirming that the slow decay of $I(t)$ is present. Moreover, within the estimated error bars, the values of $\bar{\beta}$ are the same for system sizes $L = 50, 100, 200$, indicating clearly that the condition (A) for the observation of MBL phase is not met at $W = 8$.

To check whether the condition (B) is fulfilled, we consider the flowing beta function $\beta(t)$ obtained from fitting $I(t) = at_1^{-\beta(t)}$ in the interval $t \in [t_1, 1.5t_1]$. The result, shown in the bottom panel of Fig. 3, indicates that the decay of the imbalance slows down considerably for $t \approx 150$. However, beyond that time the value of the $\beta(t)$ oscillates around the exponent $\bar{\beta}$. Therefore, we see no traces of slowing-down of the decay of imbalance at $W = 8$.

In conclusion, for $W = 8$, neither the criterion (A) nor (B) is fulfilled. Hence, we proceed to repeat our analysis for larger disorder strength $W = 10$.

Time evolution of the imbalance $I(t)$, as well as the flowing $\beta(t)$ function are shown in Fig. 4. While the decay of imbalance clearly slowed down considerably, as reflected by the values of the exponent $\bar{\beta}$ shown in Tab. II, upon the increase of disorder strength from $W = 8$ to $W = 10$, the system size dependence of $\bar{\beta}$ remains the same: the values of $\bar{\beta}$ are, within the estimated error bars, similar for $L = 50, 100, 200$, clearly not satisfying

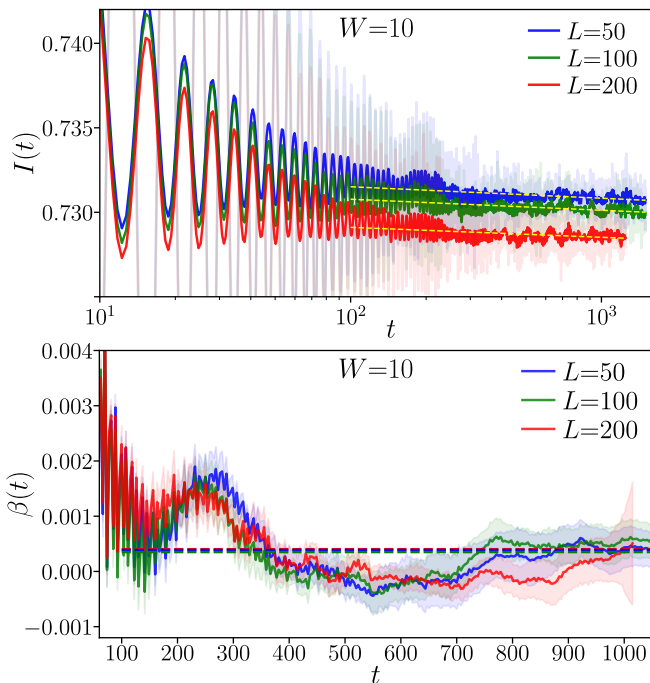


FIG. 4. Time evolution of imbalance for $W = 10$, denotation the same as in Fig. 3. Details of the simulations and fits given in Tab. II.

TABLE II. Details of numerical simulations for $W = 10$, denotations the same as in Tab. I.

	t_{\max}	χ	n_{real}	$\bar{\beta}$
$L=50$	1500	128	2000	$(4.0 \pm 0.5) \cdot 10^{-4}$
$L=100$	1500	128	2000	$(3.9 \pm 0.4) \cdot 10^{-4}$
$L=200$	1200	160	1000	$(3.5 \pm 0.6) \cdot 10^{-4}$
$L=50$	5000	192	2000	$(3.1 \pm 0.3) \cdot 10^{-4}$

the criterion (A). The flowing $\beta(t)$ function, shown in the bottom panel of Fig. 4 indicates that the decay of imbalance is relatively fast around $t \approx 200$ and then slows down considerably at $t \approx 500$ for which the value of $\beta(t)$ is vanishing. However, around $t \approx 800$ the flowing $\beta(t)$ function acquires again the value similar to $\bar{\beta}$ and the decay of imbalance persists and the criterion (B) is not met.

To make sure that our conclusions for $W = 10$ are valid, we increased the maximal time reached in our simulations to $t_{\max} = 5000$ for system size $L = 50$, the results are presented in Fig. 5. We indeed observe that the slow decay of imbalance $I(t)$ persists up to the longest time achieved in our simulation. This is exemplified by the power-law fit $I(t) \sim t^{-\bar{\beta}}$ that accurately matches the decay of imbalance in the whole interval $t \in [100, 5000]$, with the exponent $\bar{\beta}$ close to the values obtained for the shorter time intervals, see Tab. II. Moreover, the flowing $\beta(t)$ function oscillates around the value $\bar{\beta}$ in the whole interval of available times. We see no signs of the slow

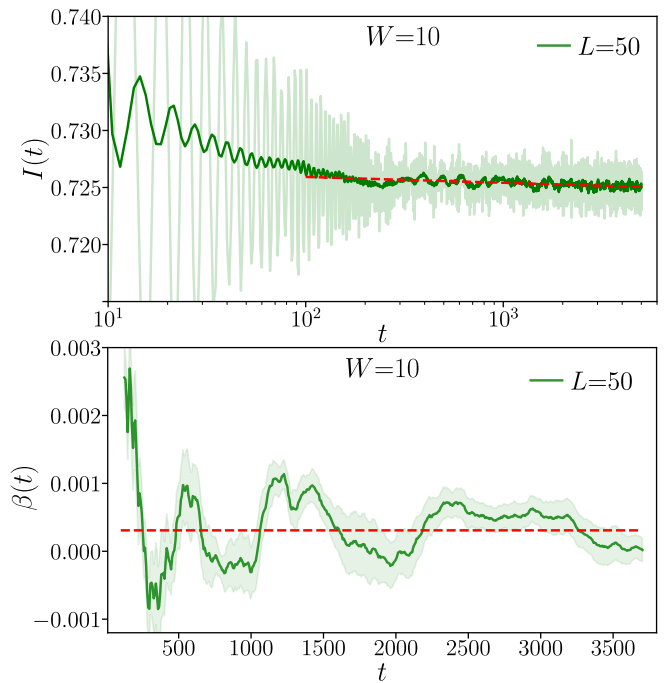


FIG. 5. Time evolution of imbalance for $W = 10$ in extended time interval, denotation the same as in Fig. 3. Details of the simulations and fits given in Tab. II.

down of decay of $I(t)$, which leads us to conclude that the criterion (B) is not fulfilled for $W = 10$.

In conclusion, we found no clear signatures of the MBL phase in results presented in this sections, even though we considered significantly larger times and disorder strengths than in earlier studies [56, 57]. One immediate question is whether we can go even further in the attempts to observe MBL phase and consider larger disorder strength W and bigger maximal time t_{\max} . The factor that limits such a continuation most severely is the slow-down of decay of $I(t)$ with W . In order to observe in a statistically significant way a decay of $I(t)$ at larger W the increase of t_{\max} should be coupled with an increase of the number of disorder realizations n_{real} . This considerably increases the resources needed for such numerical simulations. The same considerations apply to experiments with quantum many-body systems which are limited by a finite coherence time (typically limited to at most 1000 tunneling times [90] thus shorter than the times considered by us) as well as resources needed to perform disorder averages.

V. TIME EVOLUTION OF ENTANGLEMENT ENTROPY

In this section we briefly investigate dynamics of entanglement entropy in the regime of large disorder strengths and long times probed in our numerical simulations. Since the Hamiltonian (1) conserves the total magnetiza-

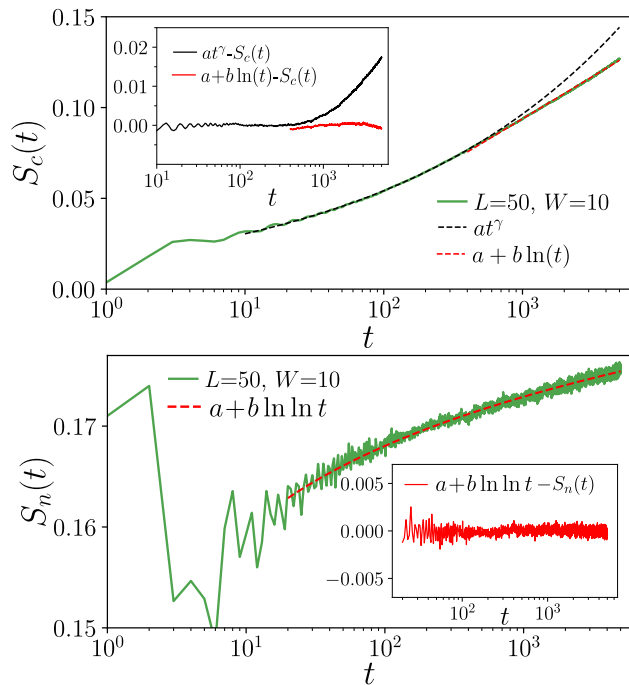


FIG. 6. Time evolution of entanglement entropy for $L = 50$ and $W = 10$. Top: configuration entanglement entropy $S_c(t)$ denoted by solid line, dashed lines denote power-law and logarithmic fits $f(t)$. The inset shows the residual $f(t) - S_c(t)$. Bottom: The number entanglement entropy $S_n(t)$ is denoted by solid line, dashed line denotes a double-logarithmic fit $f_2(t)$. The inset shows the residual $f_2(t) - S_n(t)$.

tion $\sum_{i=1}^L S_i^z$, the entanglement entropy S of subsystem A consisting of lattice sites $1, \dots, L/2$ can be written as a sum $S(t) = S_n(t) + S_c(t)$, where $S_n(t)$ is the number entropy and S_c denotes the configurational entropy [65, 76, 91, 119–121]. The number entropy is given by

$$S_n(t) = - \sum_n p(n) \ln p(n), \quad (3)$$

where $p(n)$ is the probability that $\sum_{i=1}^{L/2} S_i^z$ is equal to n . (We note that $\sum_{i=1}^{L/2} S_i^z$ is proportional to the total number of spinless fermions in subsystem A after Jordan-Wigner transformation of (1), explaining the term “number entropy”.) The configurational entropy is given by

$$S_c(t) = - \sum_n p(n) \text{Tr}[\rho(n) \ln \rho(n)], \quad (4)$$

where $\rho(n)$ is the block of the reduced density matrix in sector with $\sum_{i=1}^{L/2} S_i^z = n$.

Our results for the entanglement entropies $S_n(t)$ and $S_c(t)$ are shown in Fig. 6. The configurational entropy $S_c(t)$ is expected to grow logarithmically in time [122, 123] in the MBL regime. We observe that after an initial transient at times $t \lesssim 10$, the growth of $S_c(t)$ is well described by a power-law $S_c(t) \propto t^\gamma$ with $\gamma = 0.250(2)$ in the interval $t \in [10, 600]$. This be-

havior resembles the time dynamics of entanglement entropy observed in the ergodic regime at moderate values of disorder $W \approx 2.5$ [118]. However, at longer times, the increase of $S_c(t)$ slows down and is well fitted by $S_c(t) = a + b \ln t$ with $a = -0.04437(7)$ and $b = 0.02001(9)$ for $t \in [400, 5000]$ in agreement with expectations for the MBL regime. The growth of the number entropy is significantly slower, and is very well fitted by a double logarithmic formula $S_n(t) = a + b \ln \ln t$ with $a = 0.1496(6)$ and $b = 0.0120(3)$ in a wide regime of times $t \in [20, 5000]$. This confirms the prediction of [40, 43] for the significantly larger system size and disorder strength than tested before.

In conclusion, the slow decay of imbalance observed in Sec. IV is accompanied by a logarithmic increase of the configurational entanglement entropy $S_c(t)$ and a double logarithmic growth of the number entropy $S_n(t)$. Those quantities provide a complementary to the imbalance insight into the dynamics of the slow delocalization of the system. At the same time, they do not allow for an observation of the MBL phase in the fashion similar to the imbalance. For a localized system, one expects a saturation of $S_n(t)$ [41] instead, however, the universal level of saturation [41] is much higher than the values reached by a very slow double logarithmic growth of $S_n(t)$ observed in Fig. 6.

VI. QUASIPERIODIC SYSTEMS

In this section we attempt at observation of MBL phase in dynamics of the system with QP potential. To that end we investigate the impact of the amplitude of QP potential W^{QP} on time evolution of imbalance $I(t)$.

The results for $W^{\text{QP}} = 2, 3$ are shown in Fig. 7. The behavior of $I(t)$ is qualitatively similar to the systems with random disorder: after an initial transient, the decay of imbalance is well fitted by a power-law $I(t) \sim t^{-\bar{\beta}}$. The exponent $\bar{\beta}$ is clearly increasing with system size both for $W^{\text{QP}} = 2$ and $W^{\text{QP}} = 3$, as shown in Tab. III, suggesting that the system delocalizes in the thermodynamic limit at those values of W^{QP} and neither the criterion (A) nor (B) for observation of MBL phase is met.

The decay of imbalance $I(t)$ slows down considerably when the amplitude of the QP potential is increased to $W^{\text{QP}} = 4$ as shown in Fig. 8. The exponents $\bar{\beta}$ governing the power-law decay of imbalance for $W^{\text{QP}} = 4$ are comparable to the exponents obtained for $W = 10$ for the random disorder. However, the behavior of the running averages of $I(t)$ (shown by the solid lines in Fig. 8) is different: we observe significant oscillations around the fitted power-law decay. The pattern of those oscillations is not stable with increasing the system size, L .

This behavior changes qualitatively for $W^{\text{QP}} = 5$. For this amplitude of the QP potential we observe an emergence of a pattern of oscillations of $I(t)$ at times $t \gtrsim 200$ that remains the same when the system size is increased from $L = 12$ to $L = 200$. This is the first case for which

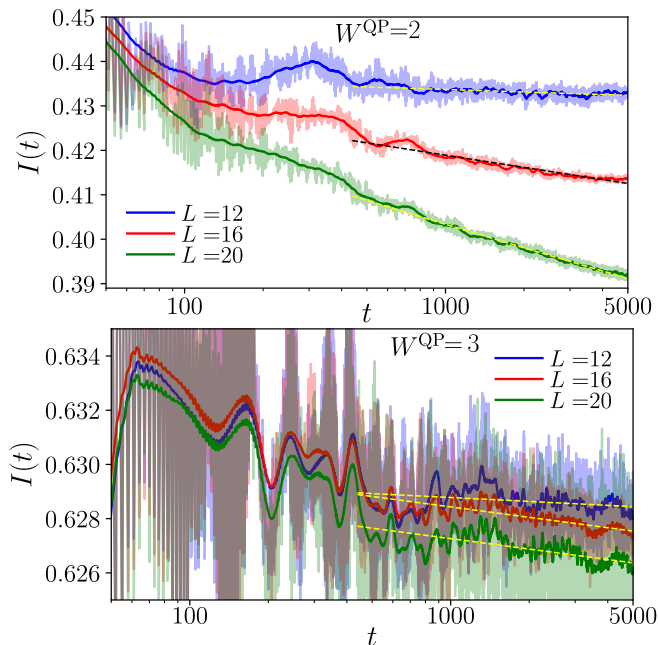


FIG. 7. Time evolution of imbalance $I(t)$ for QP potential. Top: results for the amplitude of QP potential $W^{\text{QP}} = 2$ the shaded lines denote $I(t)$ whereas the solid lines denote a running average of $I(t)$ over window $(t - 25, t + 25)$, dashed lines denote power-law fits $I(t) \sim t^{-\bar{\beta}}$ in time interval $t \in [500, 5000]$. Bottom: the same for $W^{\text{QP}} = 3$. Details of simulations are given in Tab. III

we observe that the increase of the system size does not enhance its delocalization. Instead, this result shows that the dynamics of a small system comprised of $L = 12$ sites is reproduced in the bulk of the large system of $L = 200$ sites. Such a behavior strongly suggests that the system remains MBL in the thermodynamic limit at $W^{\text{QP}} = 5$.

Two remarks are in order. Firstly, the values of the running average of $I(t)$ are not changing monotonically with L : the curve for $L = 16$ is on the top whereas that for $L = 50$ on the bottom. This is caused by the statistical fluctuations associated with the finite number of disorder realizations n_{real} as well as by the erratic changes of $2\pi kL$ modulo 2π with L that determine the number of full periods of the QP potential in the whole chain. Secondly, the emergent pattern of oscillations of $I(t)$ prevents us from determining whether the imbalance $I(t)$ slowly decays in time. Performing a power-law fit in the interval $t \in [1000, 10000]$ we have found non-vanishing values of $\bar{\beta}$ as shown in Tab. III. However, $\bar{\beta}$ changes significantly when the interval in which the fit is performed changes.

VII. CONCLUSIONS

In this work we have addressed the problem of observation of MBL. The presence of interactions gives rise to a slow dynamics towards equilibrium in strongly disor-

TABLE III. Details of numerical simulations QP potential, denotations the same as in Tab. I. The bond dimension χ is not displayed for calculation performed with the Chebyshev expansion of the evolution operator.

	t_{max}	χ	n_{real}	$\bar{\beta}$
$L=12, W^{\text{QP}}=2$	5000	-	10^6	$(1.8 \pm 0.2) \cdot 10^{-3}$
$L=16, W^{\text{QP}}=2$	5000	-	10^5	$(9.5 \pm 0.2) \cdot 10^{-3}$
$L=20, W^{\text{QP}}=2$	5000	-	$5 \cdot 10^4$	$(19.0 \pm 0.1) \cdot 10^{-3}$
$L=12, W^{\text{QP}}=3$	5000	-	10^6	$(3.3 \pm 0.4) \cdot 10^{-4}$
$L=16, W^{\text{QP}}=3$	5000	-	10^5	$(8.8 \pm 0.3) \cdot 10^{-4}$
$L=20, W^{\text{QP}}=3$	5000	-	$5 \cdot 10^4$	$(8.9 \pm 0.6) \cdot 10^{-4}$
$L=12, W^{\text{QP}}=4$	5000	-	10^6	$(2.1 \pm 0.4) \cdot 10^{-4}$
$L=16, W^{\text{QP}}=4$	5000	-	10^5	$(2.8 \pm 0.3) \cdot 10^{-4}$
$L=50, W^{\text{QP}}=4$	4000	128		$(3.0 \pm 1.3) \cdot 10^{-4}$
$L=12, W^{\text{QP}}=5$	10000	-	10^6	$(0.3 \pm 0.7) \cdot 10^{-4}$
$L=16, W^{\text{QP}}=5$	10000	-	10^5	$(1.1 \pm 0.8) \cdot 10^{-4}$
$L=50, W^{\text{QP}}=5$	4500	128	2000	-
$L=100, W^{\text{QP}}=5$	3000	128	1000	-
$L=200, W^{\text{QP}}=5$	2500	128	600	-

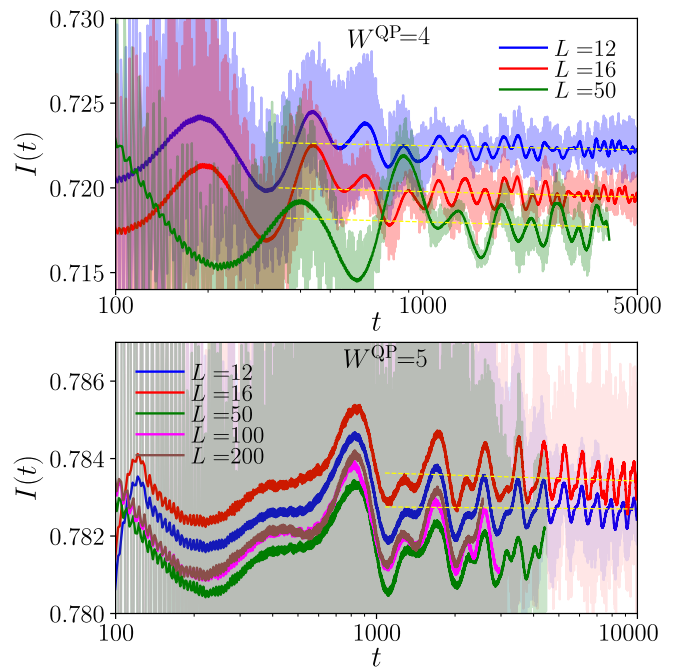


FIG. 8. Time evolution of imbalance $I(t)$ for QP potential for $W^{\text{QP}} = 4, 5$, denotation the same as in Fig. 7. Details of the simulations and fits given in Tab. III.

dered systems. This lead us to argue that an observation of even a very slow decay of correlation functions in a finite interval of time is insufficient to observe MBL.

For relatively small systems comprising of less than $L = 20$ lattice sites, we calculated time dynamics beyond the Heisenberg time which allowed us to extrapolate the results to the infinite time limit. Building on intu-

itions obtained in that way, we formulated the criteria (A) and (B) for an observation of the MBL phase. The criterion (A) requires a slowdown of the decay of density correlation functions as L^{-1} when the system size L is increased. The criterion (B) demands a saturation of correlation functions at finite times in a system size independent manner. We would like to emphasize that these criteria are neither sufficient nor necessary conditions to prove that a system is MBL. Rather, we perceive the criteria (A) and (B) as hints of whether the dynamics of a given system breaks the ergodicity or not.

Performing large scale tensor network simulations of time evolution of disordered XXZ spin chain of up to $L = 200$ sites we did not find a regime of parameters in which the criterion (A) or (B) for observation of MBL would be satisfied. For considered disorder strengths we always encountered the slow but persistent decay of imbalance hinting at a slow approach of system towards the eventually delocalized future. This conclusion was obtained even though we focused on the regime of disorder strengths lying significantly above the current estimates of the critical disorder strength for transition to MBL phase and pushed the maximal time reached in our simulations to few thousands tunneling times. We also revisited the dynamics of the entanglement entropy confirming the logarithmic growth of its configurational part and the double logarithmic increase of the number entropy in the regime of long times and large system sizes confirming predictions of [40, 43].

Finally, we investigated the time evolution of QP systems. The dynamics of quasiperiodic system is very much similar to random system at intermediate values of the amplitude W^{QP} , with a slow, power-law like decay of imbalance. However, for a stronger QP potential, at $W^{\text{QP}} = 5$, we demonstrated an emergence of a pattern of oscillations in the imbalance $I(t)$. This pattern remains stable with the increase of the system size. This qualitatively different behavior of the imbalance in a striking

fashion shows that the dynamics of QP systems at sufficiently large potential strengths becomes local. While we were eventually not able to fully exclude the decay of the imbalance in the infinite time limit, the result for QP systems appears to be not far from being sufficient to claim an observation of MBL phase. If that was the case, the criteria (A) or (B) would be met for QP systems by an oscillatory behavior of the imbalance that persists in thermodynamic limit to infinite time. In any case, our results show that the asymptotic properties of transition to MBL phase may be probed more easily in QP systems (see [114] for the analysis of QP system from the spectral perspective.)

We would like to stress that our results, especially for disordered systems, do not exclude the existence of a stable MBL phase. Rather, they provide lower bounds on time scales and disorder strengths required to observe the freezing of system dynamics in the long time limit that defines the MBL phase. Those lower bounds are relevant both for future numerical simulations of disordered systems as well as for experiments with quantum simulators, and, in particular, for observation of finite time MBL regime [44].

ACKNOWLEDGMENTS

This work would not be possible without the help of Titas Chanda who provided us with his tensor network codes and generously helped with their implementation. Thank you, Titas!. The numerical computations have been possible thanks to the support of PL-Grid Infrastructure. The TDVP simulations have been performed using ITensor library (<https://itensor.org>). This research has been supported by National Science Centre (Poland) under project 2019/35/B/ST2/00034 (J.Z.)

-
- [1] J. M. Deutsch, *Phys. Rev. A* **43**, 2046 (1991).
 - [2] M. Srednicki, *Phys. Rev. E* **50**, 888 (1994).
 - [3] M. Rigol, V. Dunjko, and M. Olshanii, *Nature* **452**, 854 EP (2008).
 - [4] I. V. Gornyi, A. D. Mirlin, and D. G. Polyakov, *Phys. Rev. Lett.* **95**, 206603 (2005).
 - [5] D. Basko, I. Aleiner, and B. Altshuler, *Ann. Phys. (NY)* **321**, 1126 (2006).
 - [6] R. Nandkishore and D. A. Huse, *Ann. Rev. Cond. Mat. Phys.* **6**, 15 (2015).
 - [7] F. Alet and N. Laflorencie, *Comptes Rendus Physique* **19**, 498 (2018).
 - [8] D. A. Abanin, E. Altman, I. Bloch, and M. Serbyn, *Rev. Mod. Phys.* **91**, 021001 (2019).
 - [9] D. A. Huse, R. Nandkishore, and V. Oganesyan, *Phys. Rev. B* **90**, 174202 (2014).
 - [10] V. Ros, M. Mueller, and A. Scardicchio, *Nuclear Physics B* **891**, 420 (2015).
 - [11] M. Serbyn, Z. Papić, and D. A. Abanin, *Phys. Rev. Lett.* **111**, 127201 (2013).
 - [12] J. Z. Imbrie, *Phys. Rev. Lett.* **117**, 027201 (2016).
 - [13] T. B. Wahl, A. Pal, and S. H. Simon, *Phys. Rev. X* **7**, 021018 (2017).
 - [14] M. Mierzejewski, M. Kozarzewski, and P. Prelovšek, *Phys. Rev. B* **97**, 064204 (2018).
 - [15] S. J. Thomson and M. Schiró, *Phys. Rev. B* **97**, 060201 (2018).
 - [16] M. Žnidarič, A. Scardicchio, and V. K. Varma, *Phys. Rev. Lett.* **117**, 040601 (2016).
 - [17] M. Serbyn, Z. Papić, and D. A. Abanin, *Phys. Rev. Lett.* **110**, 260601 (2013).
 - [18] F. Iemini, A. Russomanno, D. Rossini, A. Scardicchio, and R. Fazio, *Physical Review B* **94**, 214206 (2016).
 - [19] L. F. Santos, G. Rigolin, and C. O. Escobar, *Phys. Rev. A* **69**, 042304 (2004).
 - [20] V. Oganesyan and D. A. Huse, *Phys. Rev. B* **75**, 155111

- (2007).
- [21] A. Pal and D. A. Huse, *Phys. Rev. B* **82**, 174411 (2010).
- [22] D. J. Luitz, N. Laflorencie, and F. Alet, *Phys. Rev. B* **91**, 081103 (2015).
- [23] R. Mondaini and M. Rigol, *Phys. Rev. A* **92**, 041601 (2015).
- [24] P. Prelovšek, O. S. Barišić, and M. Žnidarič, *Phys. Rev. B* **94**, 241104 (2016).
- [25] J. Zakrzewski and D. Delande, *Phys. Rev. B* **98**, 014203 (2018).
- [26] M. Kozarzewski, P. Prelovšek, and M. Mierzejewski, *Phys. Rev. Lett.* **120**, 246602 (2018).
- [27] P. Sierant and J. Zakrzewski, *New Journal of Physics* **20**, 043032 (2018).
- [28] T. Orell, A. A. Michailidis, M. Serbyn, and M. Silveri, *Phys. Rev. B* **100**, 134504 (2019).
- [29] M. Hopjan and F. Heidrich-Meisner, *Phys. Rev. A* **101**, 063617 (2020).
- [30] P. Sierant, D. Delande, and J. Zakrzewski, *Phys. Rev. A* **95**, 021601 (2017).
- [31] Y. Bar Lev, D. R. Reichman, and Y. Sagi, *Phys. Rev. B* **94**, 201116 (2016).
- [32] X. Li, D.-L. Deng, Y.-L. Wu, and S. Das Sarma, *Phys. Rev. B* **95**, 020201 (2017).
- [33] S. Iyer, V. Oganessian, G. Refael, and D. A. Huse, *Phys. Rev. B* **87**, 134202 (2013).
- [34] V. Khemani, D. N. Sheng, and D. A. Huse, *Phys. Rev. Lett.* **119**, 075702 (2017).
- [35] N. Macé, N. Laflorencie, and F. Alet, *SciPost Phys.* **6**, 50 (2019).
- [36] J. Šuntajs, J. Bonča, T. Prosen, and L. Vidmar, *Phys. Rev. E* **102**, 062144 (2020).
- [37] P. Sierant, D. Delande, and J. Zakrzewski, *Phys. Rev. Lett.* **124**, 186601 (2020).
- [38] D. Abanin, J. Bardarson, G. De Tomasi, S. Gopalakrishnan, V. Khemani, S. Parameswaran, F. Pollmann, A. Potter, M. Serbyn, and R. Vasseur, *Annals of Physics* **427**, 168415 (2021).
- [39] R. K. Panda, A. Scardicchio, M. Schulz, S. R. Taylor, and M. Žnidarič, *EPL (Europhysics Letters)* **128**, 67003 (2020).
- [40] M. Kiefer-Emmanouilidis, R. Unanyan, M. Fleischhauer, and J. Sirker, *Phys. Rev. Lett.* **124**, 243601 (2020).
- [41] D. J. Luitz and Y. B. Lev, *Phys. Rev. B* **102**, 100202 (2020).
- [42] D. Sels and A. Polkovnikov, “Dynamical obstruction to localization in a disordered spin chain,” (2020), [arXiv:2009.04501 \[quant-ph\]](https://arxiv.org/abs/2009.04501).
- [43] M. Kiefer-Emmanouilidis, R. Unanyan, M. Fleischhauer, and J. Sirker, *Phys. Rev. B* **103**, 024203 (2021).
- [44] A. Morningstar, L. Colmenarez, V. Khemani, D. J. Luitz, and D. A. Huse, “Avalanches and many-body resonances in many-body localized systems,” (2021), [arXiv:2107.05642 \[cond-mat.dis-nn\]](https://arxiv.org/abs/2107.05642).
- [45] C. Chen, F. Burnell, and A. Chandran, *Phys. Rev. Lett.* **121**, 085701 (2018).
- [46] P. Sierant, E. G. Lazo, M. Dalmonte, A. Scardicchio, and J. Zakrzewski, *Phys. Rev. Lett.* **127**, 126603 (2021).
- [47] F. Pietracaprina, N. Macé, D. J. Luitz, and F. Alet, *SciPost Phys.* **5**, 45 (2018).
- [48] P. Sierant, M. Lewenstein, and J. Zakrzewski, *Phys. Rev. Lett.* **125**, 156601 (2020).
- [49] Schollwoeck, *Ann. Phys. (NY)* **326**, 96 (2011).
- [50] S. Paeckel, T. Köhler, A. Swoboda, S. R. Manmana, U. Schollwöck, and C. Hubig, *Annals of Physics* **411**, 167998 (2019).
- [51] G. Vidal, *Phys. Rev. Lett.* **91**, 147902 (2003).
- [52] G. Vidal, *Phys. Rev. Lett.* **93**, 040502 (2004).
- [53] J. Haegeman, J. I. Cirac, T. J. Osborne, I. Pižorn, H. Verschelde, and F. Verstraete, *Phys. Rev. Lett.* **107**, 070601 (2011).
- [54] T. Koffel, M. Lewenstein, and L. Tagliacozzo, *Phys. Rev. Lett.* **109**, 267203 (2012).
- [55] J. Haegeman, C. Lubich, I. Oseledets, B. Vandereycken, and F. Verstraete, *Phys. Rev. B* **94**, 165116 (2016).
- [56] E. V. H. Doggen, F. Schindler, K. S. Tikhonov, A. D. Mirlin, T. Neupert, D. G. Polyakov, and I. V. Gornyi, *Phys. Rev. B* **98**, 174202 (2018).
- [57] T. Chanda, P. Sierant, and J. Zakrzewski, *Phys. Rev. B* **101**, 035148 (2020).
- [58] T. Chanda, P. Sierant, and J. Zakrzewski, *Phys. Rev. Research* **2**, 032045 (2020).
- [59] J. Billy, V. Josse, Z. Zuo, A. Bernard, B. Hambrecht, P. Lugan, D. Clément, L. Sanchez-Palencia, P. Bouyer, and A. Aspect, *Nature* **453**, 891 (2008).
- [60] J. Chabé, G. Lemarié, B. Grémaud, D. Delande, P. Szriftgiser, and J. C. Garreau, *Physical Review Letters* **101** (2008), [10.1103/physrevlett.101.255702](https://arxiv.org/abs/10.1103/physrevlett.101.255702).
- [61] M. Schreiber, S. S. Hodgman, P. Bordia, H. P. Lüschen, M. H. Fischer, R. Vosk, E. Altman, U. Schneider, and I. Bloch, *Science* **349**, 842 (2015).
- [62] J. Smith, A. Lee, P. Richerme, B. Neyenhuis, P. W. Hess, P. Hauke, M. Heyl, D. A. Huse, and C. Monroe, *Nature Physics* **12**, 907 (2016).
- [63] H. P. Lüschen, P. Bordia, S. Scherg, F. Alet, E. Altman, U. Schneider, and I. Bloch, *Phys. Rev. Lett.* **119**, 260401 (2017).
- [64] T. Kohlert, S. Scherg, X. Li, H. P. Lüschen, S. Das Sarma, I. Bloch, and M. Aidelsburger, *ArXiv e-prints* (2018), [arXiv:1809.04055 \[cond-mat.quant-gas\]](https://arxiv.org/abs/1809.04055).
- [65] A. Lukin, M. Rispoli, R. Schittko, M. E. Tai, A. M. Kaufman, S. Choi, V. Khemani, J. Léonard, and M. Greiner, *Science* **364**, 256 (2019).
- [66] M. Rispoli, A. Lukin, R. Schittko, S. Kim, M. E. Tai, J. Léonard, and M. Greiner, *Nature* **573**, 385 (2019).
- [67] J. Léonard, M. Rispoli, A. Lukin, R. Schittko, S. Kim, J. Kwan, D. Sels, E. Demler, and M. Greiner, “Signatures of bath-induced quantum avalanches in a many-body-localized system,” (2020), [arXiv:2012.15270 \[cond-mat.quant-gas\]](https://arxiv.org/abs/2012.15270).
- [68] N. Y. Yao, C. R. Laumann, S. Gopalakrishnan, M. Knap, M. Müller, E. A. Demler, and M. D. Lukin, *Phys. Rev. Lett.* **113**, 243002 (2014).
- [69] M. Pino, *Phys. Rev. B* **90**, 174204 (2014).
- [70] A. L. Burin, *Phys. Rev. B* **91**, 094202 (2015).
- [71] A. L. Burin, *Phys. Rev. B* **92**, 104428 (2015).
- [72] X. Deng, G. Masella, G. Pupillo, and L. Santos, *Phys. Rev. Lett.* **125**, 010401 (2020).
- [73] P. Hauke and M. Heyl, *Phys. Rev. B* **92**, 134204 (2015).
- [74] R. Singh, R. Moessner, and D. Roy, *Phys. Rev. B* **95**, 094205 (2017).
- [75] T. Botzung, D. Vodola, P. Naldesi, M. Müller, E. Ercolessi, and G. Pupillo, *Phys. Rev. B* **100**, 155136 (2019).
- [76] P. Sierant, K. Biedroń, G. Morigi, and J. Zakrzewski, *SciPost Phys.* **7**, 8 (2019).
- [77] P. Kubala, P. Sierant, G. Morigi, and J. Zakrzewski,

- Phys. Rev. B* **103**, 174208 (2021).
- [78] E. van Nieuwenburg, Y. Baum, and G. Refael, *Proceedings of the National Academy of Sciences* **116**, 9269 (2019).
- [79] M. Schulz, C. A. Hooley, R. Moessner, and F. Pollmann, *Phys. Rev. Lett.* **122**, 040606 (2019).
- [80] L.-N. Wu and A. Eckardt, *Phys. Rev. Lett.* **123**, 030602 (2019).
- [81] S. R. Taylor, M. Schulz, F. Pollmann, and R. Moessner, *Phys. Rev. B* **102**, 054206 (2020).
- [82] E. Guardado-Sanchez, B. M. Spar, P. Schauss, R. Belyansky, J. T. Young, P. Bienias, A. V. Gorshkov, T. Iadecola, and W. S. Bakr, *Phys. Rev. X* **11**, 021036 (2021).
- [83] V. Khemani, M. Hermele, and R. Nandkishore, *Phys. Rev. B* **101**, 174204 (2020).
- [84] E. V. H. Doggen, I. V. Gornyi, and D. G. Polyakov, “Stark many-body localization: Evidence for hilbert-space shattering,” [arXiv:2012.13722](https://arxiv.org/abs/2012.13722).
- [85] R. Yao and J. Zakrzewski, *Phys. Rev. B* **102**, 104203 (2020).
- [86] R. Yao, T. Chanda, and J. Zakrzewski, “Nonergodic dynamics in disorder-free potentials,” [arXiv:2101.11061](https://arxiv.org/abs/2101.11061).
- [87] A. Y. Guo, M. C. Tran, A. M. Childs, A. V. Gorshkov, and Z.-X. Gong, *Phys. Rev. A* **102**, 010401 (2020).
- [88] T. Chanda, R. Yao, and J. Zakrzewski, *Phys. Rev. Research* **2**, 032039 (2020).
- [89] W. Morong, F. Liu, P. Becker, K. S. Collins, L. Feng, A. Kyprianidis, G. Pagano, T. You, A. V. Gorshkov, and C. Monroe, “Observation of stark many-body localization without disorder,” [arXiv:2102.07250](https://arxiv.org/abs/2102.07250).
- [90] S. Scherg, T. Kohlert, P. Sala, F. Pollmann, B. Hebbe Madhusudhana, I. Bloch, and M. Aidelsburger, *Nature Communications* **12**, 4490 (2021).
- [91] R. Yao, T. Chanda, and J. Zakrzewski, *Phys. Rev. B* **104**, 014201 (2021).
- [92] T. C. Berkelbach and D. R. Reichman, *Phys. Rev. B* **81**, 224429 (2010).
- [93] K. Agarwal, S. Gopalakrishnan, M. Knap, M. Müller, and E. Demler, *Phys. Rev. Lett.* **114**, 160401 (2015).
- [94] S. Bera, H. Schomerus, F. Heidrich-Meisner, and J. H. Bardarson, *Phys. Rev. Lett.* **115**, 046603 (2015).
- [95] T. Enss, F. Andraschko, and J. Sirker, *Phys. Rev. B* **95**, 045121 (2017).
- [96] S. Bera, G. De Tomasi, F. Weiner, and F. Evers, *Phys. Rev. Lett.* **118**, 196801 (2017).
- [97] L. Herviou, S. Bera, and J. H. Bardarson, *Phys. Rev. B* **99**, 134205 (2019).
- [98] L. A. Colmenarez, P. A. McClarty, M. Haque, and D. J. Luitz, *SciPost Physics* **7** (2019), 10.21468/scipostphys.7.5.064.
- [99] P. Sierant and J. Zakrzewski, *Phys. Rev. B* **99**, 104205 (2019).
- [100] P. Sierant and J. Zakrzewski, *Phys. Rev. B* **101**, 104201 (2020).
- [101] N. Macé, F. Alet, and N. Laflorencie, *Phys. Rev. Lett.* **123**, 180601 (2019).
- [102] N. Laflorencie, G. Lemarié, and N. Macé, *Phys. Rev. Research* **2**, 042033 (2020).
- [103] J. Gray, S. Bose, and A. Bayat, *Phys. Rev. B* **97**, 201105 (2018).
- [104] P. Naldesi, E. Ercolessi, and T. Roscilde, *SciPost Phys.* **1**, 010 (2016).
- [105] F. Setiawan, D.-L. Deng, and J. H. Pixley, *Phys. Rev. B* **96**, 104205 (2017).
- [106] Y. B. Lev, D. M. Kennes, C. Klöckner, D. R. Reichman, and C. Karrasch, *EPL (Europhysics Letters)* **119**, 37003 (2017).
- [107] S. Bera, T. Martyneć, H. Schomerus, F. Heidrich-Meisner, and J. H. Bardarson, *Annalen der Physik* **529**, 1600356 (2017).
- [108] S. A. Weidinger, S. Gopalakrishnan, and M. Knap, *Phys. Rev. B* **98**, 224205 (2018).
- [109] E. V. H. Doggen and A. D. Mirlin, *Phys. Rev. B* **100**, 104203 (2019).
- [110] F. Weiner, F. Evers, and S. Bera, *Phys. Rev. B* **100**, 104204 (2019).
- [111] H. Singh, B. Ware, R. Vasseur, and S. Gopalakrishnan, *Physical Review B* **103** (2021), 10.1103/physrevb.103.1220201.
- [112] S.-X. Zhang and H. Yao, *Phys. Rev. Lett.* **121**, 206601 (2018).
- [113] U. Agrawal, S. Gopalakrishnan, and R. Vasseur, *Nature Communications* **11**, 2225 (2020).
- [114] A. S. Aramthottil, T. Chanda, P. Sierant, and J. Zakrzewski, “Finite-size scaling analysis of many-body localization transition in quasi-periodic spin chains,” (2021), [arXiv:2109.08408](https://arxiv.org/abs/2109.08408) [cond-mat.dis-nn].
- [115] S. Nandy, F. Evers, and S. Bera, *Phys. Rev. B* **103**, 085105 (2021).
- [116] L. Vidmar, B. Krajewski, J. Bonca, and M. Mierzejewski, “Phenomenology of spectral functions in finite disordered spin chains,” (2021), [arXiv:2105.09336](https://arxiv.org/abs/2105.09336) [cond-mat.dis-nn].
- [117] H. Fehske and R. Schneider, *Computational many-particle physics* (Springer, Germany, 2008).
- [118] D. J. Luitz, N. Laflorencie, and F. Alet, *Phys. Rev. B* **93**, 060201 (2016).
- [119] N. Schuch, F. Verstraete, and J. I. Cirac, *Phys. Rev. Lett.* **92**, 087904 (2004).
- [120] N. Schuch, F. Verstraete, and J. I. Cirac, *Phys. Rev. A* **70**, 042310 (2004).
- [121] W. Donnelly, *Phys. Rev. D* **85**, 085004 (2012).
- [122] M. Žnidarič, T. Prosen, and P. Prelovšek, *Phys. Rev. B* **77**, 064426 (2008).
- [123] J. H. Bardarson, F. Pollmann, and J. E. Moore, *Phys. Rev. Lett.* **109**, 017202 (2012).